

## Cytotoxic Effects of Tanshinones from *Salvia miltiorrhiza* on Doxorubicin-Resistant Human Liver Cancer Cells

Wayne Y. W. Lee,<sup>†</sup> Chartia C. M. Cheung,<sup>†</sup> Ken W. K. Liu,<sup>†</sup> K. P. Fung,<sup>†</sup> John Wong,<sup>‡</sup> Paul B. S. Lai,<sup>§</sup> and John H. K. Yeung<sup>\*†</sup>

School of Biomedical Sciences, Faculty of Medicine, The Chinese University of Hong Kong, Shatin, New Territories, Hong Kong SAR, People's Republic of China, Department of Surgery, Prince of Wales Hospital, Shatin, New Territories, Hong Kong SAR, People's Republic of China, and Department of Surgery, Faculty of Medicine, The Chinese University of Hong Kong, Shatin, New Territories, Hong Kong SAR, People's Republic of China

Received December 7, 2009

P-Glycoprotein (Pgp) overexpression and alterations in *p53* oncogene expression are known to affect chemotherapeutic efficacy in the treatment of human hepatocellular carcinoma (HCC). The present study has demonstrated the anti-HCC potential of cryptotanshinone (**1**), dihydrotanshinone (**2**), tanshinone I (**3**), and tanshinone IIA (**4**), the active lipophilic constituents of *Salvia miltiorrhiza*, using MTT and caspase-3 activity assays and poly(ADP-ribose) polymerase cleavage in HepG2, Hep3B, and PLC/PRF/5 cells. THLE-3, a normal human immortalized liver cell line, was used to demonstrate the selective growth inhibitory effect of **3** for a HCC cell line. Compound **1** suppressed doxorubicin efflux, a process mediated by P-glycoprotein, in a Pgp-overexpressed HepG2 subclone (R-HepG2 cells). Despite its moderate cytostatic and pro-apoptotic effects and minimal influence on doxorubicin efflux, **4** provided the best synergism with doxorubicin as determined by the Combination Index, the Loewe additivity model, and the Bliss independence criterion.

Hepatocellular carcinoma (HCC) is often associated with poor diagnosis and high mortality.<sup>1</sup> For inoperable patients, chemotherapy represents the major form of treatment.<sup>2</sup> About 30–60% of HCC patients have a deficiency of *p53* activity, which may have contributed significantly in the progression of HCC.<sup>3</sup> Like *p53* deficiency, overexpression of P-glycoprotein (Pgp) led to the development of multidrug resistance in patients through its drug efflux activity.<sup>4</sup> Pgp belongs to the ABCB subfamily of the ATP-binding cassette (ABC) proteins, which requires energy provided by ATP hydrolysis for its action.<sup>5</sup> Attempts to inhibit Pgp activity, therefore eliminating or minimizing multidrug resistance by inhibition of Pgp activity, has been a focus of attention in cancer chemotherapy for over two decades. Verapamil was one of the first-generation Pgp inhibitors to undergo clinical trials, but subsequently withdrawn because of side effects and toxicity.<sup>6</sup>

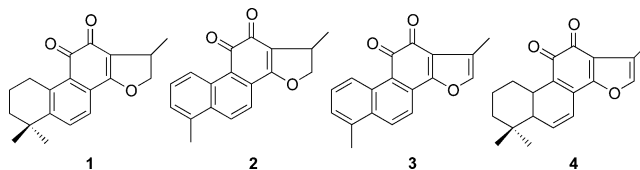
*Salvia miltiorrhiza* Bunge (Labiatae) is an herb commonly used in Chinese medicine to treat cardiovascular diseases.<sup>7,8</sup> Tanshinones are *ortho*- or *para*-naphthoquinone chromophore-containing abietane diterpenes found in the genus *Salvia*. The four major tanshinones are cryptotanshinone (**1**), dihydrotanshinone (**2**), tanshinone I (**3**), and tanshinone IIA (**4**). Investigation of this herb for other pharmacological applications, particularly its antitumor potential, began in the early 1990s.<sup>9</sup> Most recently, compound **4** was reported to inhibit growth of HCC and of breast cancer *in vivo*, respectively.<sup>10,11</sup> However, despite intermittent reports on the anti-HCC potential of tanshinones, a literature search has shown that most of the studies on the anti-HCC potential of tanshinones have been carried out in HCC cell lines with wild-type *p53* expression or Pgp deficiency. Recently, the substrate-like properties of tanshinones to Pgp have been demonstrated in the Caco-2 model and in primary rat brain microvascular endothelial cells.<sup>12,13</sup> These studies provided evidence to show the contribution of Pgp to the polarized transport of the tanshinones across the blood–brain barrier and the intestinal barrier. However, the effects of tanshinones as potential Pgp inhibitors during chemotherapy have not been addressed previously. Doxorubicin is used currently as a single agent

**Table 1.** EC<sub>50</sub> Values (μM) of Tanshinones **2** and **3** on Human Hepatocellular Carcinoma Cell Lines<sup>a</sup>

compound	HepG2	Hep3B	PLC/PRF5	R-HepG2
<b>2</b>	2.5 ± 0.4	5.5 ± 1.3	>10	4.7 ± 1.1
<b>3</b>	6.3 ± 1.1	>10	>10	>10
doxorubicin	6.1 ± 0.7	5.6 ± 1.6	>10	>10

<sup>a</sup> EC<sub>50</sub> values of compounds **1** and **4**, cisplatin, curcumin, and all-*trans*-retinoic acid were greater than 10 μM.

for systemic chemotherapy for HCC patients. Thus, the aim of this study is to investigate if the inhibitory effects of Pgp by tanshinones may provide synergism to doxorubicin cytotoxicity in a doxorubicin-resistant HCC model *in vitro*.



### Results and Discussion

Three human HCC cell lines exhibiting different *p53* genotypic profiles were used, namely, HepG2 (wild-type *p53*), Hep3B (*p53*-deleted), and PLC/PRF/5 (mutant *p53*-codon 249).<sup>14</sup> Western blot analysis confirmed the absence of *p53* in Hep3B cells, while R-HepG2, a subclone of HepG2, was shown to display a high level of Pgp expression, but not the MRP1, MRP2, and the CYP isoforms of concern (Figure S1, Supporting Information). Doxorubicin has been shown previously to exhibit transcriptional up-regulation on several CYP isoforms in rat cardiac cells (i.e., the H9c2 cell line).<sup>15</sup> The influence of MRP1, MRP2, and xenobiotic-metabolizing enzymes could therefore be excluded in this study. The MTT results indicated that up-regulation of Pgp enhanced the drug resistance of R-HepG2 cells to doxorubicin (Table 1), which was partly reversed by verapamil pretreatment (data not shown).

Tanshinones **2** and **3** and doxorubicin showed potent growth-inhibitory effects against various HCC cell lines, as summarized in Table 1. Indeed, compounds **1**–**4** induced growth inhibition in a monotonic concentration-dependent manner, and the mode of

\* To whom correspondence should be addressed. Tel: +852-26096864. Fax: +852-26035139. E-mail: johnyeung@cuhk.edu.hk.

<sup>†</sup> School of Biomedical Sciences, The Chinese University of Hong Kong.

<sup>‡</sup> Department of Surgery, Prince of Wales Hospital.

<sup>§</sup> Department of Surgery, The Chinese University of Hong Kong.

inhibition by these agents was cell-type dependent. Doxorubicin exerted potent growth inhibitory effects on HepG2 and Hep3B cells but was much less effective on PLC/PRF/5 and R-HepG2 cells, in which mutant *p53* and Pgp overexpression enhanced drug resistance to doxorubicin *in vitro*.<sup>16,17</sup> Among the tanshinones studied, the growth inhibitory effects of **2** and **3** were comparable to that of doxorubicin in the four HCC cell lines, which suggested that **2** and **3** are effective in the presence of Pgp overexpression and different *p53* genotypic profiles. However, such drug-resistance features played a more important role in the growth inhibitory effects of **1** and **4**. R-HepG2 cells were still sensitive to **1** and **4** when compared with doxorubicin. Other tested chemicals, including cisplatin, curcumin, and all-*trans*-retinoic acid, suppressed the growth of HepG2 cells less effectively, and their inhibitory effect was limited by *p53* deficiency/alteration and Pgp overexpression. Interestingly, R-HepG2 cells were more sensitive to **1** and cisplatin (22.5% and 11.4% more potent, respectively) than HepG2 cells. In this study, the effectiveness of the cytostatic effect of the four tanshinones was also investigated on THLE-3, immortalized human liver cells, again using the MTT assay. The EC<sub>50</sub> values of the cytostatic effects for **1–4** on THLE-3 cells were 22.9 ± 1.2, 6.5 ± 1.3, 74.1 ± 1.3, and 57.5 ± 1.2 μM (*n* = 3), respectively.

Apart from inhibiting the growth of HCC cancer cell lines, tanshinones **1–4** caused apoptotic cell death, as indicated by poly(ADP-ribose) polymerase (PARP) cleavage, in HepG2 cells in a concentration-dependent manner (Figure S2, Supporting Information). The result was consistent with findings in the MTT assay. Hep3B, PLC/PRF/5, and R-HepG2 cells demonstrated different susceptibility to the tanshinone-induced PARP cleavage. Hep3B cells were completely insensitive (*p* > 0.05, *n* = 3) to tanshinone-induced PARP cleavage, while PLC/PRF/5 cells and R-HepG2 cells were sensitive only to **2** and **3** in a concentration-dependent manner. Moreover, a caspase-3 activity assay was used to evaluate the pro-apoptotic effect of **1–4** on the HCC cell lines. The four tanshinones and etoposide (positive control) activated caspase-3 in HepG2 cells (Figure 1A) concentration dependently. All four tanshinones caused activation of caspase-3 at 25 μM, with **3** and **4** being somewhat effective. Compound **2** was the most potent, increasing caspase-3 activity by 2-fold at 6.25 μM. Similar to the results of the PARP cleavage assay, Hep3B cells were not responsive to the tanshinone-induced caspase-3 activation or the effect of etoposide (data not shown). Compared with HepG2 and Hep3B cells, **1–4** showed only a moderate caspase-3-activating effect on PLC/PRF/5 cells. Compound **2** (6.25 μM) activated caspase-3 by 2.5-fold, but this effect was not sustained at higher concentrations. A monotonic concentration-dependent trend of caspase-3 activation was observed in PLC/PRF/5 cells treated with **1**, but was not statistically significant (Figure 1B). Taken together, the cytostatic and cytotoxic effects of compounds **1–4**, like other chemotherapeutics, were susceptible to the Pgp and *p53* intervention. Compound **2** was among the only tanshinones that retained considerable cytostatic and cytotoxic effects in cell lines with Pgp overexpression or *p53* deletion.

To examine the regulatory effect of tanshinones **1–4** on Pgp expression, MRP1, and MRP2, HepG2 cells were incubated with **1–4** (25 μM) for 24 h. Western blot analysis indicated that the tanshinones did not down- or up-regulate the expression of the drug transporter proteins (data not shown). Thus, any influence by tanshinone treatment on the expression of transporters in this study can be eliminated. Verapamil, a prototype Pgp inhibitor, reduced doxorubicin efflux in R-HepG2 cells concentration dependently, with compounds **1** and **2** showing similar effects (Figures S3A and S3B, Supporting Information). The modulating effect of **1** was greater than that of verapamil and was concentration-dependent (Figure S3C, Supporting Information). Indomethacin, a MRP1 inhibitor, was used to test the involvement of MRP1 in doxorubicin efflux in R-HepG2 cells, but showed no significant effect at 10 to

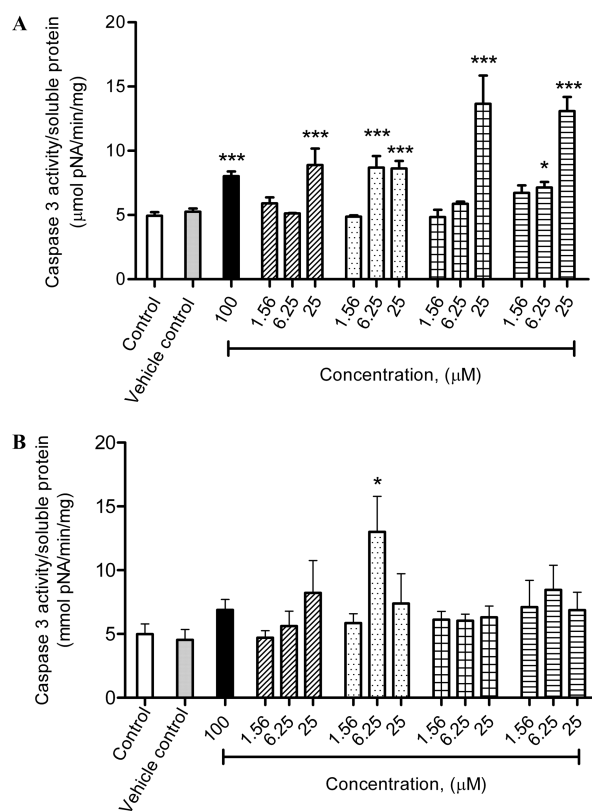


**Figure 1.** Effects of the tanshinones, compounds **1** (diagonal), **2** (dotted), **3** (checked), **4** (striped), or etoposide (■), on the activation of caspase-3 in HepG2 (A), and PLC/PRF/5 (B) cell lines (mean ± SEM, *n* = 4) (\**p* < 0.05 and \*\*\**p* < 0.001 indicate significance compared with control groups).

100 μM (*p* > 0.05, *n* = 3). However, the presence of 100 μM indomethacin greatly reduced the inhibitory effect of verapamil and **1** on Pgp-mediated doxorubicin efflux (Figure S3D, Supporting Information). Indomethacin has previously been shown to reverse drug efflux through inhibiting glutathione *S*-transferase (GST) or acting as a binding-site competitor;<sup>18</sup> thus, this enzyme may be a target site for the enhancing action on doxorubicin efflux by indomethacin. Ethacrynic acid, a nonselective GST inhibitor, was found to reduce GST activity by 2-fold (Figure S3E, Supporting Information). The effect of ethacrynic acid on doxorubicin efflux was comparable to that rendered by indomethacin (Figure S3F, Supporting Information).

The tanshinone–doxorubicin interaction on the growth inhibition of R-HepG2 cells, as evaluated by a Combination Index,<sup>19</sup> is summarized in Table 2. The results showed that the type of interaction varied at different concentrations of tanshinones and effect level. Compound **4** showed the greatest synergy in doxorubicin-induced growth inhibition, with a synergism (0.3 < CI < 0.7) and strong synergism (0.1 < CI < 0.3) at 25 and 6.25 μM, respectively. Compounds **1** at 25 μM and **3** at 6.25 μM, enhanced the cytostatic effect of doxorubicin at the 50% effect level. Index of interaction against net Loewe additivity plot (Figure 2A) showed that **1**, like **4**, possesses obvious Loewe synergism in the concentration range 6.25 to 25 μM, but also showed considerable Loewe antagonism in the concentrations range 1.56 to 6.25 μM. Compounds **2** and **3** behaved as antagonists in this study. Similar findings were observed in the Bliss 3D plot (Figure 2B), where **1** and **4** showed Bliss synergism (*E*(BI) – *E*(Exp) < 1), whereas **2** and **3** were Bliss antagonists (*E*(BI) – *E*(Exp) > 1).

In this study, the cytostatic and cytotoxic effects of tanshinones **1–4** were reduced in the presence of *p53* deficiency or mutation and Pgp overexpression. However, the growth-inhibitory effect of the tanshinones was still greater than that produced by doxorubicin.

**Table 2.** Combination Effects of the Tanshinones on Doxorubicin in R-HepG2 Cells<sup>a</sup>

compound	concentration ( $\mu\text{M}$ )	Combination Index value at		<i>n</i>
		EC <sub>20</sub>	EC <sub>50</sub>	
1	1.56	1.30	ND <sup>b</sup>	6
	6.25	1.81	ND <sup>b</sup>	3
	25	7.21	0.74	3
2	0.39	ND <sup>b</sup>	ND <sup>b</sup>	4
	1.56	1.73	ND <sup>b</sup>	6
	6.25	5.21	1.34	6
3	0.39	ND <sup>b</sup>	ND <sup>b</sup>	4
	1.56	ND <sup>b</sup>	ND <sup>b</sup>	6
	6.25	3.21	0.31	6
4	1.56	0.55	ND <sup>b</sup>	4
	6.25	0.50	0.14	4
	25	1.99	0.51	4

<sup>a</sup> Growth inhibition was calculated using the MTT assay. <sup>b</sup> Not determined at the designated EC values.

The data are the first evidence to show the cytostatic effects of 2–4 in a normal liver cell line, in which the therapeutic window for 3 was greater than that of 2 and 4. MTT assay, PARP cleavage, and caspase-3 activity were utilized to investigate the susceptibility of different HCC cell lines to tanshinones-induced apoptosis. Results in the present study substantiate the importance of wild-type *p53* expression in tanshinones-induced apoptosis, which has been observed in PLC/PRF/5 cells and in *p53* wild-type SMMC-7721 cells.<sup>20</sup> However, 2 and 3 showed growth-inhibitory effects in Hep3B cells, a *p53*-deficient HCC cell line, through activation of *p38* MAPK, triggering cell cycle arrest in Hep3B cells.<sup>21</sup> The vital role of ROS-mediated *p38* MAPK activation has been identified in tanshinones-induced apoptosis in HepG2 cells.<sup>22</sup> Taken together, these findings indirectly indicate that the cytostatic and/or cytotoxic effects of 2 and 3 may be *p53*-independent. It appears that 2 is a potent and effective cytostatic agent through induction of apoptosis, followed by 3, 4, and 1. However, the low cytostatic selectivity of 1, 2, and 4 on cancer cell lines may limit their potential as systemic chemotherapeutics against HCC.

Flow cytometric analysis revealed the reversal effect of 1 and verapamil on Pgp-mediated doxorubicin efflux. However, it should be noted that the R-HepG2 cell line has been established and maintained through a stepwise increase in the concentration of doxorubicin in HepG2 cells. Therefore, the expression of other drug transporters and drug metabolizing enzymes not addressed in this study may be altered and thus may interfere with subsequent experimentation and interpretation. Although the transcript levels of CYPs 1A2, 2C9, 2C19, 2D6, 2E1, and 3A4 in HepG2 cells were much lower than that in cryopreserved primary human hepatocytes, the regulatory activity of aryl hydrocarbon receptor (AhR) on CYP1A2 and pregnane X receptor (PXR) CYP3A4 in response to corresponding agonists has been demonstrated in HepG2 cells.<sup>23</sup> In addition to CYP3A4, activated pregnane X receptor binding to the nuclear receptor has also been shown to regulate MDR1 (gene encoding Pgp) and glutathione *S*-transferase.<sup>24,25</sup> This may explain the correlation of enhanced GST activity and Pgp overexpression in the R-HepG2 cells. However, the significance of GST up-regulation coupled with Pgp overexpression is unclear but merits further investigations.

In terms of reversing drug resistance to doxorubicin through Pgp modulation, 1 appeared to be an encouraging compound (Figures S3A and S3C, Supporting Information). However, when different mathematical models (Table 2 and Figure 2, A and B) were used to calculate synergism of the tanshinones and doxorubicin in cell growth inhibition, 4 provided the strongest synergism with doxorubicin. The mathematical models used in this study represent different modes of drug–drug interaction. The Bliss independence criterion assumes the two interacting agents act independently from one another, while the Loewe additivity model and Combination

Index assume the two interacting agents act on the same biological site.<sup>26</sup> The mechanism(s) underlying doxorubicin-induced cytotoxicity and growth inhibition is/are unclear, but possible mechanisms include inhibition of topoisomerase II and apoptosis induction through oxidative stress<sup>22,27,28</sup> and disruption of metaphase–anaphase transition.<sup>29,30</sup> The complexity of the mechanisms involved makes the interpretation of calculation of drug–drug interactions from equations more difficult, and there are pros and cons of using different approaches for calculating synergy.<sup>31</sup> The median-effect method by Chou and Talalay (i.e., the Combination Index used in the present study) has been widely cited since its publication. However, it is limited for a mutually nonexclusive case (i.e., the assumption for the Bliss independence criterion). Thus, the Bliss independence criterion was used to confirm if tanshinones are synergistic to doxorubicin. The results showed that the synergistic effect of 4 on doxorubicin exists over a wider concentration range (1.56 to 25  $\mu\text{M}$ ), but this synergy may be independent from Pgp modulation. In addition to its cytotoxic and cytostatic effects at different concentrations on various HCC cell lines, the mathematical models clearly showed that 4 can enhance the retention of doxorubicin in Pgp overexpressed HCC cells. However, the poor oral bioavailability<sup>13</sup> of 4 may require the drug be administered parenterally to enhance its effectiveness as an adjuvant agent.

In conclusion, the anti-HCC effects of tanshinones 1–4 have been demonstrated in different HCC cell lines of different *p53* profiles and Pgp overexpression. The tanshinones also showed synergism to a doxorubicin-resistant HCC cell line. The intrinsic cytostatic effects of the tanshinones to cause apoptosis in cancer cells and their synergistic interactions with established anticancer drugs may provide significant contribution to their anti-HCC potential.

## Experimental Section

**General Experimental Procedures.** Three HCC cell lines (HepG2, Hep3B, and PLC/PRF/5) and an immortalized human liver cell line (THLE-3) were purchased from the American Type Culture Collection (ATCC, Rockville, MD). The HepG2 cell line was cultured in minimum essential medium (Gibco, Grand Island, NY), and the Hep3B and PLC/PRF/5 cell lines were cultured in Dulbecco's modified Eagle medium (Gibco) with 1% nonessential amino acid, supplemented with 10% fetal bovine serum, 50 U/mL penicillin, and 50  $\mu\text{g}/\text{mL}$  streptomycin (Gibco). THLE-3 was cultured according to manufacturer's instructions (ATCC, Rockville, MD) using the BEGM bullet kit (Lonza, Walkersville, MD). The development of a drug-resistant HepG2 cell line toward doxorubicin, a clone named R-HepG2, has been described previously.<sup>32</sup> This cell line was cultured in RPMI 1640 (Gibco) supplemented with 10% fetal bovine serum, 50 U/mL penicillin, and 50  $\mu\text{g}/\text{mL}$  streptomycin. Doxorubicin (1.2  $\mu\text{M}$ ) was added to maintain sustainable Pgp expression. All cell lines were incubated at 37 °C in 5% CO<sub>2</sub>.

**Cytostatic Effects of Tanshinones 1–4 on the Cell Lines Used.** Cell proliferation was determined by the MTT assay. Briefly, cells ( $9 \times 10^3$  per well) were plated in 96-well plates. After drug incubation for the desired period, 100  $\mu\text{L}$  of 3-(4,5-dimethyl-2-thiazolyl)-2,5-diphenyltetrazolium bromide (MTT, 0.5 mg/mL) was added to each well and the plate incubated at 37 °C for another 3 h. The end products, formazan crystals, were dissolved in DMSO and quantified spectrophotometrically at 570 nm using a microplate reader. Cells without the addition of test compounds served as vehicle control.

**Calculation of Drug Interactions.** Drug interactions were evaluated by the Combination Index method originally described by Chou and Talalay,<sup>19</sup> the Loewe additivity method, and the Bliss independence criterion method. The development of the theorem of Combination Index is based on the median-effect equation, which is derived from the law of mass action:

$$\text{CI} = (D)_1/(D_x)_1 + (D)_2/(D_x)_2 \quad (1)$$

where  $(D)_1$  and  $(D)_2$  are the concentrations of the two test compounds added together at which  $x\%$  inhibition is also achieved.  $\text{CI} < 1$ , = 1, and  $>1$  indicate synergism, additivity, and antagonism, respectively. Two classic models for a drug combination study, namely,



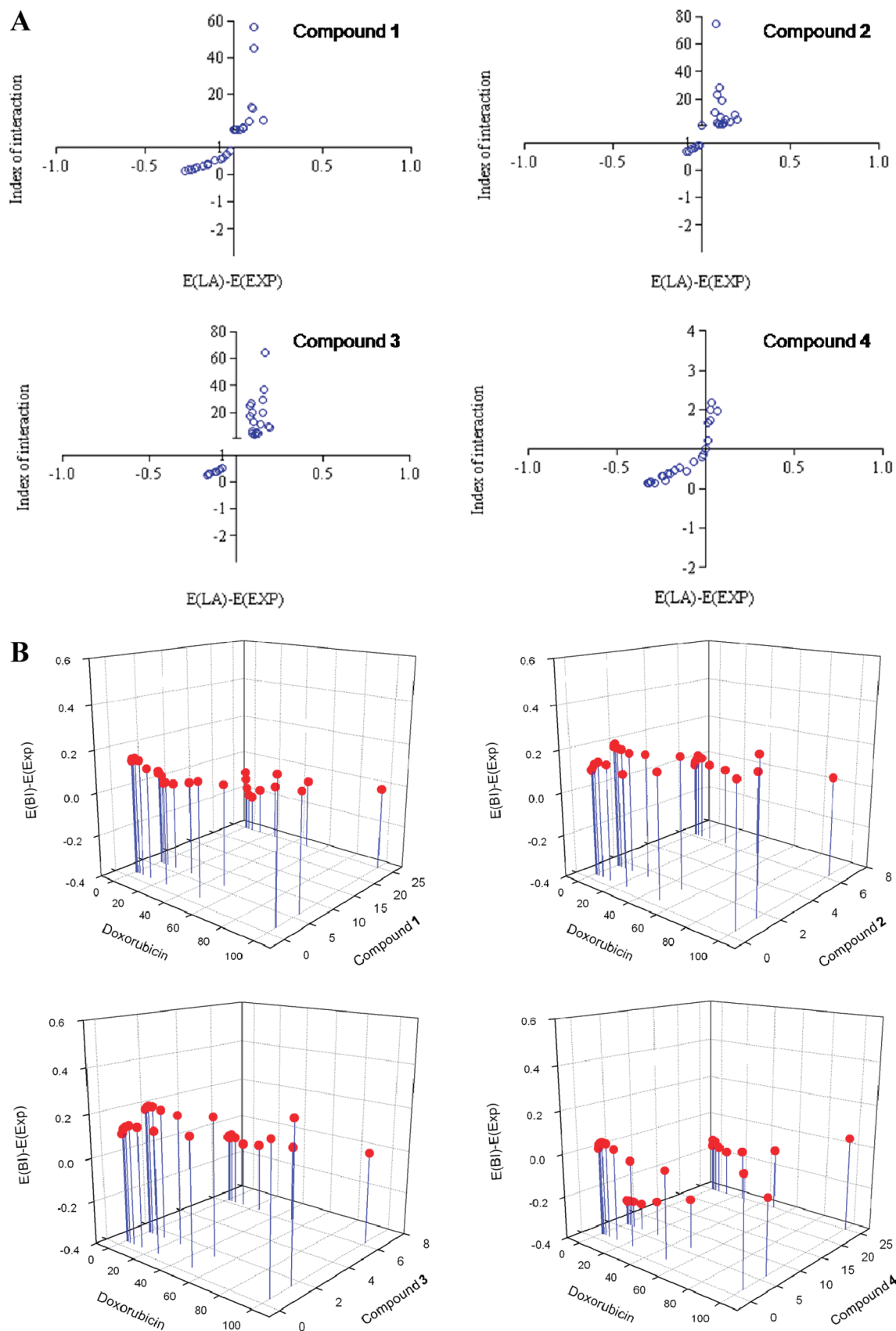


**Figure 2.** Correlation between the index of interaction and the effect difference between calculated Loewe additivity and experimental data (A). 3D plot comparison of the calculated Bliss independence and experimental data (B).

the Loewe additivity model and the Bliss independence criterion, were applied to validate the result of the Combination Index determination further.<sup>31</sup> The calculation of the Loewe additivity

combination effect and the Bliss independence combination effect and construction of corresponding correlation plots and 3D interaction plots were performed using CombiTool (Sühnel Lab, Leibniz

Institute for Age Research, Germany) and Origin 7.0 (OriginLab Corporation), respectively. The Loewe additivity model assumes all the substances of interest in the mixture act on the same biological site, and the Loewe additivity equation is derived from the mass conservation law. Therefore, an index of interaction less than 1 denotes Loewe synergism, while an index of interaction greater than 1 denotes Loewe antagonism and an index of interaction equal to 1 means Loewe additivity (i.e., zero interaction). The Bliss independence criterion assumes a totally different mode of action of the substances of concern. Thus, if the experimental combination effect is greater than the expected Bliss value, the interaction is considered as Bliss synergism and *vice versa*.

Cytotoxic effects of tanshinones 1–4 in the three HCC cell lines was determined by a caspase-3 activity assay (Caspase-3 Assay Kit, Colorimetric, Sigma) and a PARP cleavage study. After 24 h tanshinone treatment, cells ( $1 \times 10^7$ ) were lysed in 100  $\mu$ L of lysis buffer for 2 h at 4 °C. The lysed cells were centrifuged at 16000g for 10 min at 4 °C. The supernatant was collected and mixed with assay buffer and caspase-3 substrate (Ac-DEVE-pNA) according to the manufacturer's instruction. Release of colorimetric pNA from the substrate as the result of caspase-3 activity was determined at 405 nm. The concentration of total soluble protein was determined using the BCA Protein Assay Kit (Thermo Scientific, Rockford, IL). PARP cleavage was determined by western blotting, with 20  $\mu$ g of soluble protein prepared in lysis buffer (pH 7.5) (50 mM Trizma base, 100 mM NaCl, 5 mM EDTA, 67 mM sodium pyrophosphate, and 1% Triton X-100) supplemented with protease inhibitor cocktail (Roche, Germany), subjected to 8% SDS-PAGE, and transferred to nitrocellulose membranes (Pall, Ann Arbor, MI). The blocked membrane was incubated in 1:1000 primary antibody against PARP overnight at 4 °C, followed by 1 h incubation in 1:2000 HRP-goat anti-rabbit IgG at room temperature (Cell Signaling, Beverly, MA). Blots were developed using the ECL chemiluminescence detection reagent (Amersham Bioscience, Little Chalfont, UK). The membranes were then reprobbed with  $\beta$ -actin as loading reference. Intensity of the blots was quantified with Scion software. Similar procedures of western blotting were conducted to determine the expression of Pgp, MRP1, MRP2, and the five most abundant CYP isoforms (CYP1A2, 2C9, 2D6, 2E1, and 3A4) in HepG2 cells.

The retention of doxorubicin by either HepG2 or Pgp-overexpressed-HepG2 cells was determined by flow cytometry. In short,  $1 \times 10^6$  cells per mL of phosphate-buffered saline (PBS, Gibco) were prepared in a 1.5 mL microcentrifuge tube. Modulators at the desired concentration were added to the cell suspension and left for 15 min preincubation at 37 °C in a thermomixer with gentle shaking (Eppendorf, Barkhausenweg, Hamburg, Germany). Doxorubicin (10  $\mu$ M) was added to each tube for a further 1.5 h of incubation in the mixer. The cells were collected by centrifugation at 400g for 5 min and resuspended in 500  $\mu$ L of chilled PBS. The suspension was subjected to flow cytometric analysis with excitation at 470 nm and emission at 585 nm. Expo32 software was used for data analysis.

To determine the activity of glutathione S-transferase, cells grown in a 75 cm<sup>2</sup> flask, with a seeding density of  $2 \times 10^6$  per flask, for 48 h were pretreated with ethacrynic acid (40  $\mu$ M) or DMSO (vehicle control) for 1 h. The cells were washed twice with PBS and collected by trypsinization. Cell pellets were homogenized in chilled homogenizing buffer (100 mM potassium phosphate, 2 mM EDTA, pH 7.0) and centrifuged at 10000g for 15 min at 4 °C. The supernatant was collected for a GST activity assay, while the pellet was dissolved in 0.9% NaCl for a protein assay. Glutathione S-transferase activity was determined as previously described.<sup>33</sup> Briefly, the supernatant was mixed with reaction buffer (100 mM sodium phosphate, 0.1 mM EDTA, pH 6.5), 30 mM glutathione, and 15 mM CDNB. The formation of GSH conjugate to CDNB was monitored at 340 nm using a plate reader to obtain at least five time points. Results were calculated using a CDNB extinction coefficient of 0.00505  $\mu$ M. One unit of GST converted 1.0 nmol of CDNB with GSH per minute at 25 °C in a 1 mL reaction mixture.

**Chemicals.** Compounds 1–4 were purchased from Chengdu Cogon Biotech Co., Ltd. (Chengdu, Sichuan, People's Republic of China). Their purities were 98%, as determined by HPLC-MS. In-house HPLC was utilized to monitor the content of the tanshinones routinely as previously described.<sup>28</sup> Stock solutions of these compounds were freshly prepared daily in DMSO, in which the final concentration of the solvent was 0.25% (v/v) throughout all experiments. Doxorubicin and primary antibodies against MRP1 and

MRP2 were purchased from Alexis Biochemicals (San Diego, CA). Primary antibody against Pgp was purchased from Calbiochem (Damstadt, Germany). Primary antibodies against  $\beta$ -actin and GADPH were purchased from Santa Cruz Biotechnology, Inc. (Santa Cruz, CA). Primary antibodies against CYP1A2, CYP2C8/9/19, CYP2D6, and CYP2E1 were purchased from Chemicon (Billerica, MA). Primary antibody against CYP3A4 was purchased from Thermo Fisher Scientific Inc. (Rockford, IL). Primary antibody against p53 was purchased from BD Bioscience (Franklin Lakes, NJ). Unless otherwise specified, all other chemicals used in this study were purchased from Sigma Chemical Co. (St. Louis, MO).

**Statistical Analysis.** Statistical analysis was carried out by Student's *t* test/one-way or two-way analysis of variance (ANOVA) followed by Tukey's post hoc test, where appropriate. All data are presented as the means  $\pm$  standard error of the mean. A value of  $p < 0.05$  was considered statistically significant.

**Acknowledgment.** We thank Mrs. C. H. Huey Jenny for expert technical assistance and advice. W.Y.W.L. and C.C.M.C. are recipients of postgraduate studentships (Division of Pharmacology) from the Chinese University of Hong Kong. The work described in this paper was partly supported by a grant from the Research Grants Council of the Hong Kong Special Administrative Region, People's Republic of China (project no. CUHK4517/06 M).

**Supporting Information Available:** Protein expression p53, transporters, and CYPs in different human hepatocellular carcinoma cell lines. Tanshinones-induced PARP cleavage in HepG2, Hep3B, PLC/PRF/5, and R-HepG2 cells. Effects of tanshinones on the retention of doxorubicin in HepG2 and R-HepG2 cells. This information is available free of charge via the Internet at <http://pubs.acs.org>.

## References and Notes

- Parkin, D. M.; Pisani, P.; Ferlay, J. *CA Cancer J. Clin.* **1999**, *49*, 33–64.
- Schwartz, J. D.; Beutler, A. S. *Anticancer Drugs* **2004**, *15*, 439–452.
- Martin, J.; Dufour, J. F. *World J. Gastroenterol.* **2008**, *14*, 1720–1733.
- Borst, P.; Jonkers, J.; Rottenberg, S. *Cell Cycle* **2007**, *6*, 2782–2787.
- Glavinas, H.; Krajcsi, P.; Cserepes, J.; Sarkadi, B. *Curr. Drug Delivery* **2004**, *1*, 27–42.
- Liang, X. J.; Aszalos, A. *Curr. Drug Targets* **2006**, *7*, 911–921.
- Xu, D. S. *Dan Shen (Radix Salviae Miltorrhizae): Biology and Application*; Beijing Science Press: Beijing, 1990.
- Wang, X. H.; Morris-Natschke, S. L.; Lee, K. H. *Med. Res. Rev.* **2007**, *27*, 133–148.
- Wu, W. L.; Chang, W. L.; Chen, C. F. *Am. J. Chin. Med.* **1991**, *19*, 207–216.
- Huang, X. Y.; Wang, L.; Huang, Z. L.; Zheng, Q.; Li, Q. S.; Tang, Z. Y. *J. Cancer Res. Clin. Oncol.* **2009**, *135*, 1245–1255.
- Wang, X.; Wei, Y.; Yuan, S.; Liu, G.; Lu, Y.; Zhang, J. *Int. J. Cancer* **2005**, *116*, 799–807.
- Chen, X.; Zhou, Z. W.; Xue, C. C.; Li, X. X.; Zhou, S. F. *Xenobiotica* **2007**, *37*, 635–678.
- Yu, X. Y.; Lin, S. G.; Zhou, Z. W.; Chen, X.; Liang, J.; Liu, P. Q.; Duan, W.; Chowbay, B.; Wen, J. Y.; Li, C. G.; Zhou, S. F. *Curr. Drug Metab.* **2007**, *8*, 325–340.
- Bressac, B.; Galvin, K. M.; Liang, T. J.; Isselbacher, K. J.; Wands, J. R.; Ozturk, M. *Proc. Natl. Acad. Sci. U. S. A.* **1990**, *87*, 1973–1977.
- Zordoky, B. N.; El-Kadi, A. O. *Vasc. Pharmacol.* **2008**, *49*, 166–172.
- Chan, K. T.; Lung, M. L. *Cancer Chemother. Pharmacol.* **2004**, *53*, 519–526.
- Lee, T. K.; Lau, T. C.; Ng, I. O. *Cancer Chemother. Pharmacol.* **2002**, *49*, 78–86.
- Draper, M. P.; Martell, R. L.; Levy, S. B. *Br. J. Cancer* **1997**, *75*, 810–815.
- Chou, T. C.; Talalay, P. *Adv. Enzyme Regul.* **1984**, *22*, 27–55.
- Yuan, S. L.; Wei, Y. Q.; Wang, X. J.; Xiao, F.; Li, S. F.; Zhang, J. *World J. Gastroenterol.* **2004**, *10*, 2024–2028.
- Gao, Y.; Lin, L. P.; Zhu, C. H.; Chen, Y.; Hou, Y. T.; Ding, J. *Cancer Biol. Ther.* **2006**, *5*, 978–985.
- Lee, W. Y.; Liu, K. W.; Yeung, J. H. *Cancer Lett.* **2009**, *285*, 46–57.
- Westerink, W. M.; Schoonen, W. G. *Toxicol. In Vitro* **2007**, *21*, 1581–1591.
- Knight, T. R.; Choudhuri, S.; Klaassen, C. D. *Toxicol. Sci.* **2008**, *106*, 329–338.

- (25) Synold, T. W.; Dussault, I.; Forman, B. M. *Nat. Med.* **2001**, *7*, 584–590.
- (26) Goldoni, M.; Johansson, C. *Toxicol. In Vitro* **2007**, *21*, 759–769.
- (27) Binaschi, M.; Bigioni, M.; Cipollone, A.; Rossi, C.; Goso, C.; Maggi, C. A.; Capranico, G.; Animati, F. *Curr. Med. Chem. Anticancer Agents* **2001**, *1*, 113–130.
- (28) Kotamraju, S.; Kalivendi, S. V.; Konorev, E.; Chitambar, C. R.; Joseph, J.; Kalyanaraman, B. *Methods Enzymol.* **2004**, *378*, 362–382.
- (29) Lee, W. Y.; Chiu, L. C.; Yeung, J. H. *Food Chem. Toxicol.* **2008**, *46*, 328–338.
- (30) Zhou, L.; Chan, W. K.; Xu, N.; Xiao, K.; Luo, H.; Luo, K. Q.; Chang, D. C. *Life Sci.* **2008**, *83*, 394–403.
- (31) Greco, W. R.; Bravo, G.; Parsons, J. C. *Pharmacol. Rev.* **1995**, *47*, 331–385.
- (32) Li, Y. C.; Fung, K. P.; Kwok, T. T.; Lee, C. Y.; Suen, Y. K.; Kong, S. K. *Chemotherapy* **2004**, *50*, 55–62.
- (33) Yeung, J. H.; Or, P. M. *Food Chem. Toxicol.* **2007**, *45*, 953–961.

NP900792P